EuroSDR-Project
Commission 1 “Radiometric aspects of digital photogrammetric images”

Final Report

Report by

Eija Honkavaara and Lauri Markelin
Remote Sensing and Photogrammetry – Finnish Geodetic Institute, Masala

Roman Arbiol and Lucas Martínez
Institut Cartogràfic de Catalunya, Catalonia

Abstract

This report presents the results and conclusions of the EuroSDR project "Radiometric aspects of digital photogrammetric images" that was carried out during 2008-2011. The project was a European-wide multi-site research project, where the participants represented stakeholders of photogrammetric data in National Mapping Agencies, software development and research. The project began with a review phase, which consisted of a literature review and a questionnaire to the stakeholders of photogrammetric data. The review indicated excellent radiometric potential of the novel imaging systems, but also revealed many shortcomings in the radiometric processing lines. The second phase was an empirical investigation, for which radiometrically controlled flight campaigns were carried out in Finland and in Spain using the Leica Geosystems ADS40 and Intergraph DMC large-format photogrammetric cameras. The investigations considered vicarious radiometric calibration and validation of sensors, spatial resolution assessment, radiometric processing of photogrammetric image blocks and practical applications. The results proved the stability and quality of evaluated imaging systems with respect to radiometry and optical system. The first new-generation methods for reflectance image production and equalization of photogrammetric image blocks provided promising results and were also functional from the productivity and usability points of view. For reflectance images, an accuracy of up to 5% was obtained without need of ground reference measurements. Application oriented results indicated that automatic interpretation methods will benefit from the optimal use of radiometrically accurate stereoscopic photogrammetric imagery. Many improvements are still needed for the processing chains in order to obtain full advantage of the radiometric potential of photogrammetric sensors.

During the project, the quantitative radiometric processing in photogrammetric processing lines was not mature technology at all. Operational applications used qualitative and statistical methods in assessing and processing the radiometry, and the output image products were mainly used in visual interpretation. The major emphasis in this investigation was to consider the radiometry from the quantitative point of view. This report summarizes many points of view to the radiometric processing and all the evaluated methods can be further developed and implemented as automated tools in modern photogrammetric processes of National Mapping Agencies in the future.

1 Introduction

A special advantage of the new digital large-format photogrammetric imagery is a high-quality multi-spectral radiometry. The high-quality radiometry opens up new prospects for the utilization of the photogrammetric imagery, but also requires new approaches for the data processing. The rigorous treatment of image radiometry is a new issue in photogrammetric processing chains. To investigate these issues, the European Spatial Data Research organization (EuroSDR) launched a project called "Radiometric aspects of digital photogrammetric images" in May 2008.

1.1 Objectives of the Project

The fundamental objectives of this EuroSDR project were as follows:

1. Improve knowledge on radiometric aspects of digital photogrammetric cameras.

2. Review existing methods and procedures for radiometric image processing

3. Compare and share operative solutions through a comparison of these techniques on a same test data set.

4. Analyse the benefit of radiometric calibration and correction in different applications (classification, quantitative remote sensing, change detection etc.).

1.2 Phases of the project

The project was realized in two phases. In the first phase, a review was made on radiometric aspects of digital photogrammetric images based on literature and a questionnaire to stakeholders of photogrammetric processes. In the second phase, a comparative, multi-site, empirical investigation was conducted.

1.3 Participants

In total, six National Mapping Agencies (NMA), one company and seven research participants participated the project (Table 1).

Participant	Organization	Role	Phases
Institut Cartogràfic de Catalunya (ICC)	NMA	Software developer, Data provider, Data user, Research	1,2
Institut Géographique National, France (IGN), Ecole Nationale des Sciences Géographiques (IGN/ENSG) and Laboratoire MATIS (IGN/MATIS)	NMA	Sensor manufacturer, Software developer, Data provider, Data user, Research	1, 2
National Survey and Cadastre, Denmark (KMS)	NMA	Data user	1
National Land Survey, Finland (NLS)	NMA	Data provider, Data user	1
Ordnance Survey, Great Britain (OS)	NMA	Data provider, Data user	1
Swiss Federal Office of Topography (Swisstopo)	NMA	Data provider, Data user	1, 2
ReSe Applications Schläpfer, Switzerland (ReSe)	Company	Software, Consultant, Research	1, 2
Finnish Geodetic Institute, Finland (FGI)	Research	Research	1, 2
Institut für Geoinformatik und Fernerkundung, Universität Osnabrück (IGF)	University	Research	1
University of Helsinki (UH)	University	Research	2
University of Eastern Finland (UEF)	University	Research	2
Instituto de Desarrollo Regional – Universidad de Castilla La Mancha (IDR-UCLM)	University	Research	2
Centre de Recerca Ecològica i Aplicacions Forestals – Universitat Autònoma de Barcelona (CREAF-UAB)	University	Research	2

Universitat de Barcelona (UB)	University	Research	2
Universitat Politècnica de Catalunya (UPC)	University	Research	2
Servei Meteorològic de Catalunya (SMC)	Meteorological Institute	Research	2

Table 1. Participants of the project

1.4 Publications

Results of the project have been presented in several scientific articles and reports. This final report will present some of the highlights of the results, and the summary and conclusions of the project; detailed results are given in the detailed publications. In this report, these publications will be referred using bold Roman numbers.

General descriptions of the project

I. Arbiol, R., Martinez, L., 2009. ICC-Banyoles 2008 Campaign in the framework of EUROSDR Radiometry Project. Project description and preliminary results. Proceedings of XI Geomatic Week, Barcelona. 3 - 5 March.

http://www.icc.cat/cat/content/download/48926/340513/file/banyoles_2008.pdf

II. Arbiol, R., Martínez, L., 2010. ICC EuroSDR Banyoles08 research activities. International Calibration and Orientation Workshop EuroCOW 2010. Castelldefels (Barcelona), 10–12 Feb.

http://www.ideg.es/page.php?id=1360

http://www.icc.cat/cat/content/download/20086/64380/file/11_ICC%20EUROSDR%20BANYOLES08%20RESEARCH%20ACTIVITIES.pdf

III. Honkavaara, E., Arbiol, R., Markelin, L., Martinez L., Cramer, M., Korpela, I., Bovet, S., Thom, C., Chandelier, L., Ilves, R., Klonus, S., Reulke, R., Marshall, P., Tabor, M., Schläpfer, D., and N. Veje, 2009. Status report of the EuroSDR project "Radiometric aspects of digital photogrammetric airborne images". Proceedings of the ISPRS Hannover Workshop 2009, Hannover, Germany, June 2-5, 2009.

http://www.isprs.org/proceedings/XXXVIII/1_4_7-W5/paper/Honkavaara-154.pdf

IV. Honkavaara, E., Arbiol, R., Markelin, L., Martinez, L., Bovet, S., Bredif, M., Chandelier, L., Heikkinen, V., Korpela, I., Lelegard, L., Pérez, F., Schläpfer, D., Tokola, T., 2011. The EuroSDR project "Radiometric aspects of digital photogrammetric images" – Results of the empirical phase. In Proceedings of the ISPRS Hannover Workshop 2011, June 14-17, 2011, Hannover, 8 pages.

http://www.isprs.org/proceedings/XXXVIII/4-W19/paper/Contribution172.pdf

Theory of image radiometry and results of Phase I

V. Honkavaara, E., Arbiol, R., Markelin, L., Martinez, L., Cramer, M., Bovet, S., Chandelier, L., Ilves, R., Klonus, S., Marshall, P., Schläpfer, D., Tabor, M., Thom, C., and N. Veje, 2009.

Digital airborne photogrammetry – A new tool for quantitative remote sensing? – A state-of-the-art review on radiometric aspects of digital photogrammetric images. Remote Sensing, Vol. 1, 577-605.

http://dx.doi.org/10.3390/rs1030577

Calibration

VI. Honkavaara, E., Nurminen, K., Markelin, L., Suomalainen, J., Ilves, R., 2011. Calibrating and validating multispectral photogrammetric 3D imaging system at a permanent test site – Case study with an Intergraph DMC. Photogrammetric Record, 26 (134), 229-249.

http://dx.doi.org/10.1111/j.1477-9730.2011.00634.x

VII. Markelin, L., Honkavaara, E., Hakala, T., Suomalainen and J., Peltoniemi, J., 2010. Radiometric stability assessment of an airborne photogrammetric sensor in a test field. ISPRS Journal of Photogrammetry and Remote Sensing, 65(4): 409-421.

http://dx.doi.org/doi:10.1016/j.isprsjprs.2010.05.003

VIII. Martínez, L., Arbiol, R., Pérez, F., 2010. Casi characterization and atmospheric correction for EuroSDR Banyoles08 dataset. International Calibration and Orientation Workshop EuroCOW 2010. Castelldefels (Barcelona).

http://www.ideg.es/page.php?id=1360

IX. Martinez, L., Soler, M.E., Pérez, F., Arbiol, R., 2011. Efecto de la atmósfera en la resolución óptica de la Z/I Digital Mapping Camera. Revista de Teledetección, nº 35, p. 32-40.

http://www.aet.org.es/revistas/revista35/Numero35_04.pdf

http://www.icc.cat/cat/content/download/48052/330277/file/2011_RET_35_Martinez.pdf

Atmospheric correction of images

X. Markelin, L., Honkavaara, E., Beisl, U. and Korpela, I., 2010. Validation of the radiometric processing chain of the Leica ADS40 airborne photogrammetric sensor. International Archives of Photogrammetry, Remote Sensing and Spatial Information Sciences, 38(7A): 145-150.

http://www.isprs.org/proceedings/XXXVIII/part7/a/pdf/145_XXXVIII-part7A.pdf

XI. Markelin, L., Honkavaara, E., Schläpfer, D., Bovet, S. and Korpela, I., 2012. Assessment of radiometric correction methods for ADS40 imagery. PFG 3/2012: 251-266

http://dx.doi.org/10.1127/1432-8364/2012/0115

Results of applications using reflectance signatures

XII. Heikkinen, V., Korpela, I., Tokola, T., Honkavaara, E. and Parkkinen, J., 2011. An SVM classification of tree species radiometric signatures based on the Leica ADS40 sensor. IEEE

Transactions on Geoscience and Remote Sensing. IEEE Transactions on Geoscience and Remote Sensing, 49(11): 4539-4551.

http://dx.doi.org/10.1109/TGRS.2011.2141143

XIII. Korpela, I., Heikkinen, V., Honkavaara, E., Rohrbach, F. and Tokola, T., 2011. Variation and directional anisotropy of reflectance at the crown scale - Implications for tree species classification in digital aerial images. Remote Sensing of Environment 115 (8), 2062-2074.

http://dx.doi.org/10.1016/j.rse.2011.04.008

XIV. Martínez, L., Pérez, F., Arbiol, R., and Magariños, A., 2012. Development of NDVI WMS geoservice from reflectance DMC imagery at ICC. International Calibration and Orientation Workshop EuroCOW 2012. Castelldefels (Barcelona), 8–10 Feb.

http://www.ideg.es/page.php?id=1360

Reports of individual participants

XV. Bovet, S., 2010. Phase2 empirical evaluation of ADS data Product generation with the Hyytiälä dataset at Swisstopo. Project report.

XVI. Brédif, M., Lelégard, L., 2010. Study of DMC panchro images resolution. Project report.

XVII. Chandelier, L., 2010. Performance test of IGN radiometric aerial triangulation. Project report.

XVIII. A. Comerón, A., Muñoz, C., Md Reba, N., Rocadenbosch, F., Sicard, M., Tomás, S., 2008. Banyoles 2008 Campaign, UPC Lidar Measurements.

XIX. Cunilera , J., Martinez, L., 2010. Banyoles 2008 Campaign, SMC Report.

XX. Markelin, L., 2012. Weather conditions during the 23rd Aug, 1st Sep and 25th Sep 2008 Campaigns in Finland.

XXI. Markelin, L., 2012. Supplementary results for the article XI: "Assessment of Radiometric Correction Methods for ADS40 Imagery".

XXII. Schläpfer, D., 2010. The Potential of Atmospheric and Topographic Correction for ADS40/80. EuroSDR project report.

XXIII. Sola, Y., Lorente, J., Campmany, E., 2008. Banyoles 2008 Campaign, UB Report.

XXIV. Phase I questionnaire.

2 Phase I – Review

2.1 Objectives

The objective of the review phase was to provide the necessary background information on the radiometric aspects of photogrammetric images, and it consisted of a literature review and a questionnaire to various stakeholders. The questionnaire was considered crucial, because existing literature covered only partially the modern photogrammetric process and it did not give information about radiometric processing in operational processes. Detailed results of the review are given in **V**.

Objectives of the questionnaire were to:

1. obtain a picture of the actual situation;
2. detect main weaknesses of existing digital camera radiometric processing;
3. look for main trends on existing and future development in this field;
4. learn what the advantages of better radiometric processing are and find which applications ask for better radiometric processing.

The questions were classified into five themes: sensor, calibration, image collection, post-processing and utilization of the images. For each theme, the questions were further divided into questions related to the current situation and to the desired situation. The questionnaire is given in **XXIV**.

2.2 Outcome of questionnaire

The questionnaire was delivered to several large and medium format photogrammetric sensor manufacturers, photogrammetric software providers, NMAs and Universities in October 2008.

The organizations that replied to the query are shown in Table 1. The widest response was obtained from NMAs, most of which are both data providers and users; some also have their own software development (IGN, ICC), and IGN is manufacturing its own sensor. ReSe is a software company behind the atmospheric correction software ATCOR for spaceborne and airborne scanner images, and is specialized in processing and utilization of imaging spectroscopy data in particular. In total, five responses were obtained from data providers, six from data users, one from a sensor manufacturer, three from radiometric software developers, and two from research organizations.

The major conclusions of the questionnaire were that improvements were requested for the entire process: sensors, calibration, data collection, data post-processing and data utilization. The fundamental problems could be listed as follows:

1. there was insufficient information on the radiometric processing chain,
2. radiometric processing chains were inadequate and
3. standards were missing, including methods, calibration, reference targets, and terminology.

The basic radiometric end products requested by image users were true color images and reflectance images. The expected benefit of a more accurate radiometric processing includes a more automatic and efficient image post-processing, better visual image quality, more accurate and automatic interpretation, and the quantitative use of data.

The results indicated that it is necessary to identify the interest groups related to the photogrammetric process. The fundamental processes are the sensor manufacturing, software development, photo-

grammetric image acquisition, photogrammetric image product generation (orthophotos, stereomodels), applications and research. The main interest groups are data users, data providers, sensor manufacturers, software developers and research organizations. Each interest group can be further divided into different subclasses based on the tasks they undertake. For example, the data user can undertake all phases of the process (sensor manufacturing, image collection, software development, image product generation, applications) or he can concentrate on only the application. Each of these groups has a different possibility to manage, influence or discover the details of the radiometric processing chain. Important interest groups are presented in Table 2; the interest groups of the participants of the questionnaire are shaded.

Type	Sensor manufacturing	Software development	Data collection	Image products	Applications	Research
U1	x	x	x	x	x	(x)
U2		x	x	x	x	(x)
U3			x	x	x	(x)
U4				x	x	(x)
U5					x	(x)
P1	x	x	x			(x)
P2	x	x	x	x		(x)
P3			x			(x)
P4			x	x		(x)
R1						x
SW1		x				(x)
M1	x	x				(x)

Table 2. Various interest groups dealing with image radiometry. The groups that are covered in the questionnaire are shaded. U1-U5: different classes of users, P1-P4: different classes of image producers. R1: research; SW1: software developer; M1: sensor manufacturer.

All data users expressed concern about the traceability of the radiometry. An important comment comes from the organization that purchases all the imagery: "We lack information on the entire data processing and also lack technical information on the integrated sensor system (e.g. position of GNSS/IMU related to the image sensor) and how the resulting image frame is computed". The traceability and comparability of data collected with various sensors is especially a problem for users that order images. For the IGN, who is manufacturing its own sensor, all relevant information is available when needed.

2.3 Fundamental equations of image radiometry

As a part of the review, the fundamental equations related to the radiometric processing of photogrammetric images were identified. These are summarized below and more details are given in **V** and referenced literature.

Fundamental output products of the radiometric correction process are reflectance images and true color images:

- Reflectance images contain information about the reflection characteristics of objects in scene and they have a lot of potential in automatic and quantitative interpretation applications. Fundamental steps in the reflectance image generation are the compensation of sensor

artefacts (based on sensor calibration), atmospheric effects as well as object bidirectional reflection behavior.

- In true color images, colors are presented in a way which is attractive for the human visual system. In this case, the standard way to proceed is to transform the images to a standard color space, such as the CIE-XYZ color space. Colorimetric calibration is useful for applications where images are interpreted visually, but only applicable for images collected in blue, green and red wavelengths. For color infrared images this approach is not functional.

In this study we emphasize the reflectance image generation. The rigorous color image production requires the same steps and an additional colorimetric calibration; Martínez et al. (2007) gives more details about this process.

In high resolution photogrammetric imaging, the elementary components of radiance entering the sensor (L_{at_sensor}) are the radiance components from the object of interest, that is to say, the surface-reflected solar radiance (L_s), the reflected skylight (L_{sky}), the reflected background radiance (L_{bg}) and the radiance reflected first by the background objects and then by the atmosphere (L_{bg_multi}); the adjacency effect (L_{adj}) and atmospheric path radiance (L_{atm}) are radiance components that do not carry any information of the object of interest (Schott, 2007):

$$L_{at\_sensor} = L_s + L_{sky} + L_{bg} + L_{bg\_multi} + L_{adj} + L_{atm}. \quad (1)$$

The digital grey value (DN) at a given pixel, after dark pixel subtraction is applied, can be given as follows:

$$DN = GA_d \Omega \tau \int_0^\infty L_{at-sensor}(\lambda) S(\lambda) d\lambda \,, \quad (2)$$

where G is system gain, A_d is the area of the detector, Ω is the lens solid angle (aperture), τ is the integration or exposure time, $S(\lambda)$ is the system level spectral response, and λ is the wavelength. The sensor model in Equation 2 is given for the Intergraph DMC (Ryan and Pagnutti, 2009). This equation is referred as a sensor model in this report.

In practice, the band averaged values are used. For each band the relationship between the DN and band averaged at-sensor radiance ($\overline{L}$) can be given as follows:

$$\overline{L} = K' \frac{\tau}{f_{number}^{\,2}} DN \,, \quad (3)$$

where K' is the calibration coefficient needed for each band and f_{number} is f-number (aperture). Ideally, K' is needed for each band, but for example in the case of DMC, K' is determined for various apertures due to the insuffient stability (Ryan and Pagnutti, 2009).

In practice, the most significant components that are taken into account by atmospheric correction methods are L_s, L_{sky} and L_{atm}. The reflectance where atmospheric influences are corrected can be given as:

$$\rho = \pi (L_{at-sensor} - L_{atm})(1 - s\rho') / (S\tau_s \tau_v) \,, \quad (4)$$

where ρ is the surface reflectance, s is the spherical albedo of atmosphere (the fraction of the upward radiance that is backscattered by the atmosphere), ρ' is the average reflectance of the surrounding area, $(1-s\rho')$ is the term to take into account the multiple scattering, S is the mean solar irradiance in surface ($S=E_\lambda^0 \cos\theta_s$) and τ_s and τ_v are the transmittance in solar and viewing paths, respectively. (**V**; Richter and Schläpfer, 2002; Besil et al., 2008)

One of the important aspects related to the radiometry of photogrammetric images is the anisotropy of object reflectance. This phenomenon means that the reflection of object is a function of the viewing and illumination geometries. This can be modelled by the bidirectional reflectance distribution fubction (BRDF):

$$\rho(\theta_i,\varphi_i,\theta_r,\varphi_r) = \frac{L(\theta_i,\varphi_i,\theta_r,\varphi_r)}{E(\theta_i,\varphi_i)}\,, \tag{5}$$

where $L(\theta_i,\varphi_i,\theta_r,\varphi_r)$ is the radiance reflected by the object, $E(\theta_i,\varphi_i)$ is the irradiance at object, θ_i,φ_i are the zenith and azimuth angles of incident light and θ_r,φ_r are the zenith and azimuth angles of reflected light (Schaepman-Strub et al., 2005; von Schönermark et al., 2004).

2.4 Objectives of the empirical phase

Based on the results of the questionnaire and the potential of the available image materials, the following topics were selected as the general objectives of the empirical phase:

1. Radiometric calibration and characterization
2. Spatial resolution assessment
3. Reflectance image calculation and image block equalization
4. Color enhancement of the calibrated data
5. Application oriented studies

These topics cover the fundamental processes of the radiometric processing chain.

Objectives 1 and 2 are related to validation and calibration of the imaging sensor and system, which should be carried out on a regular basis (e.g. yearly) to ensure the quality of the imaging system. These aspects should be considered also in the acceptance testing of a purchased new sensor system. The use of a test field for calibration purpose, instead of using either laboratory calibration or calibration on the actual mapping task itself (on-the-job calibration), is known as vicarious calibration in the remote sensing community, and used also in this report.

Objectives 3 and 4 are related to the producing of output images that are used in various applications, such as stereo mapping and automatic change detection. The methods used by NMAs have to be suitable for processing of huge amounts of image data (tens to hundreds of thousands of km^2 every year). Radiometric correction is crucial in order to produce accurate, high-quality image data products. The key requirements for these processes include efficiency (fast processing, no ground reference targets), usability aspects (simplicity of use, automatic selection of parameters), reliability and accuracy. In this project, the color enhancement part was not covered.

The last objective is related to the fact that the radiometric processing level and quality of image data has influences in applications. In this project the application oriented studies concerned the NDVI data layer generation and tree species classification.

3 Phase II: Empirical investigation – Set-up

3.1 Empirical image data

In summer and autumn 2008, radiometrically controlled test flights were conducted in Catalonia and in Finland. Details of the campaigns are described below.

3.1.1 Integrated DMC and CASI test flight in Banyoles

ICC executed extensive radiometric test flights with a DMC and the Compact Airborne Spectrographic Imager (CASI) in Banyoles in 15 July, 2008 (Figure 1) (**I, II**). The imagery was collected from 820, 1125, 2250 and 4500 m flying altitudes, providing GSDs of 7.5 cm, 10 cm, 20 cm and 30 cm. Various manmade reflectance targets as well as several artificial and natural stable covers were available around the test field, including a lake; two groups carried out the radiance and reflectance ground-truth data acquisition with spectroradiometers. In addition, a Siemens star was installed in the test field. Atmospheric state was directly measured by several groups, instruments and techniques: an atmospheric Lidar provided aerosol profiles and two automatic sun tracking photometers provided column integrated values of Aerosol Optical Thickness (AOT) for the optical spectrum. Atmospheric information simultaneous to the airborne sensors overflight was also available. The atmospheric conditions were excellent with an AOT at 500 nm of less than 0.1 (**XVIII**, **XIX, XXIII**).

Figure 1. Airborne imagery and ground truth data collected on 15 July, 2008 in Banyoles. ICC test field is deployed on a football field.

The scientific objectives of this campaign were:

1. Radiometric calibration of a DMC by the radiance and the reflectance methods. Validation with radiometric targets. Radiance method will be performed with the simultaneous acquisition of CASI.

2. Spectral characterization of CASI regarding bandwidth and smiling effect. Comparison with laboratory results.

3. Atmospheric correction of CASI imagery with aerosol distribution and load, and water vapor derivation by an inversion method. Validation with radiometric targets and atmospheric measurements.

4. Atmospheric correction of DMC images by using CASI derived atmosphere parameters. Validation with radiometric targets.

5. Colorimetric calibration of DMC towards CIE standard color space. Validation with radiometric targets.

6. Resolution studies by means of a Siemens star and edge targets. Study of the relationship between atmosphere state and resolution. Comparison with computer radiative transfer simulations.

7. Application of DMC radiance and reflectance images to remote sensing studies.

3.1.2 DMC test flights in Sjökulla

The National Land Survey of Finland (NLS) carried out an acceptance testing of their new DMC on 1 and 25 September 2008 at the Sjökulla test field of the FGI (Figure 2) (Honkavaara et al., 2008; Honkavaara, 2008; **VI**). The flying height was 500 m above the ground level, which provided a 5 cm GSD. The reflectance reference targets included six permanent bidirectional reflectance factor (BRF) targets of gravel available at the test field, three transportable BRF targets and several natural covers. By using the BRF-calibrated targets, it is possible to obtain accurate reference reflectance for different viewing/illumination geometry (Suomalainen et al., 2009). In-situ groundtruth measurements were carried out using an ASD (Analytical Spectral Devices) field spectrometer during the flights. A Siemens star, edge target and line bar targets were available for the spatial resolution evaluations. Visibility measurements were carried out at the Helsinki-Vantaa airport at 30 km distance from the test area; in both flights the visibility was good, approximately 30-50 km (**XX**).

Figure 2. Left: Flight lines in Sjökulla on 1 September, 2008. Right: Radiometric and spatial resolution targets at Sjökulla test field. B1: Black gravel; R1: Red gravel; B2a: Black gravel, version a; B2b: Black gravel, version b; G: Grey gravel; W2: White gravel; P20, P30, P50: portable reference reflectance targets with nominal reflectance of 0.20m 0.30 and 0.50.

The scientific objectives of this campaign were:

1. Absolute radiometric calibration of the DMC by the reflectance method.

2. Spatial resolution studies of the DMC using Siemens star, edge targets and resolution bar targets.

3. Evaluation of the influences of various exposure and aperture settings on the radiometric performance and spatial resolution of the DMC.

4. Evaluation of the BRF measurement potential of the DMC.

The many difficulties in this campaign show the typical challenges of radiometrically controlled imaging campaign. The acceptance testing was scheduled for the beginning of August. Unfortunately the weather conditions were too poor in August, so the campaign could not be executed before September; the field measurement team was ready for takeoff for more than one month and three field campaigns were carried out unnecessarily. In the first successful airborne campaign the sensor settings were not optimum, and the images were saturated in worst cases already with a reflectance value of 0.25. To obtain unsaturated images and to allow proper acceptance testing, a second campaign was carried out by the end of September. The field measurement team was not prepared for this campaign and the spectrometer was not available, so only reflectance targets were installed in the test field.

3.1.3 Integrated ADS40/ALS50 test flight in Hyytiälä

The test flight with ADS40 (SH 52) and ALS50 (Airborne Laser Scanner) was carried out at the Hyytiälä forestry test field in co-operation with Leica Geosystems, University of Helsinki, University of Eastern Finland, Estonian Land Board and FGI (Figure 3). The test site was 3300 m x 8500 m in size and it contains more than 200 forest plots and over 15000 trees that have been measured for position and basic variables, in different forest conditions (density, age, species mixture, silvicultural history) (Korpela et al. **XIII**). A state-of-the-art weather station for atmospheric research runs at the area of interest (SMEAR II, AERONET) (Holben et al., 1998; Hari and Kulmala, 2005). FGI's BRF calibrated reflectance targets and a Siemens star were installed at the test field. The reflectance/radiance of the targets as well as various homogeneous land covers (asphalt, sand, gravel, grass) were measured by FGI and Leica Geosystems using spectroradiometers. ADS40 data was collected with the uncompressed mode from 1000, 2000, 3000 and 4000 m flying altitudes providing GSDs of 10 cm, 20 cm, 30 cm and 40 cm. Atmospheric conditions were not as perfect as in Banyoels campaign, with an AOT at 500 nm of 0.14 - 0.18 (**XX**).

The scientific objectives of this campaign were:

1. Absolute radiometric calibration of the ADS40 by the reflectance method and comparisons to laboratory calibration.

2. Evaluation of the performance of radiometric correction methods.

3. Evaluation of the BRF measurement potential of the ADS40.

4. Spatial resolution studies of the ADS40 using Siemens star.

5. Evaluation of influence of radiometric correction level in forestry applications.

6. Further objectives of the entire campaign include the radiometric calibration of ALS50 and its utilization in forestry applications, which is out of scope of this project.

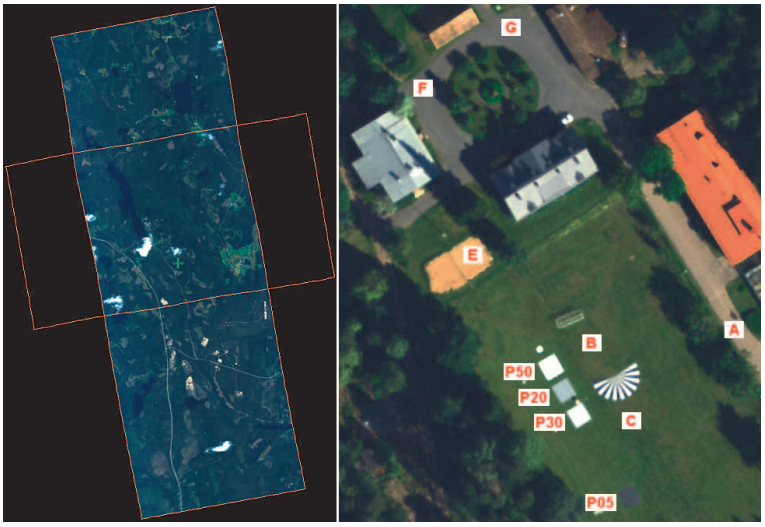

Figure 3. Left: 4 km flying height ADS40 image block from the Hyytiälä area on 23 August, 2008. Right: Reference measurements in Hyytiälä.

The varying weather conditions caused problems in this campaign as well. The field measurement team was ready for takeoff for one week; the campaign could be carried out in one Saturday morning. The positive feature of this campaign was that continuously operating sun photometer and weather station are permanent equipment at the test site, which helped greatly the field operations. After the airborne campaign clouds entered rapidly to the test site, thus complete BRF characterization of the natural targets at the test site could not be carried out.

Objective	DMC Banyoles	DMC-Sjökulla	ADS Hyytiälä	Participant, method
Radiometric calibration and characterization of the sensor/system	x			ICC: CASI+6S
		x	x	FGI: MODTRAN4
			x	FGI:ATCOR-4
			x	RESE: ATCOR-4
Spatial resolution assessment	x			IGN/MATIS: Siemens star
	x			IGN/MATIS: Image
	x			ICC: Siemens star
		x		FGI: Siemens star
		x		FGI: Resolving Power (RP) targets
Reflectance image generation, radiometric block adjustment	x			IGN: Pepita
		x		FGI: Empirical line method
			x	FGI: XPro
			x	FGI: ATCOR-4
			x	Rese: ATCOR-4
			x	Swisstopo: XPro
Applications	x			ICC: NDVI
			x	UH, UEF: tree species classification

Table 3. Summary of objectives, methods and participants in empirical study.

3.2 Processing of the data

The participants of the empirical phase included three National Mapping Agencies (NMAs), one company providing atmospheric correction software and eight research participants (Table 1). The data was delivered to some additional parties, but they did not return any results. Summary of the objectives of the empirical study and how these were covered by the project participants, data sets and approaches are given in Table 3. The methods are described in the following sections.

4 Phase II – Radiometric calibration and characterization of the sensor/system

Radiometric calibration determines the radiometric response of an imaging system. The central task is the determination of absolute and relative radiometric response (Beisl, 2006; Ryan and Pagnutti, 2009). The absolute radiometric calibration determines for each channel the calibration coefficients (Equation 3). The relative radiometric calibration normalizes the output of the sensor so that a uniform response is obtained in the entire image area; the corrections are determined at least for sensitivity differences of individual cells of a detector array, defect pixels, light falloff and dark signal. In addition, spectral and colorimetric models and PSF are necessary information in radiometric processing, and various non-uniformities are of interest to achieve high absolute calibration accuracies. The exact parameterization is always system dependent.

For airborne sensors, the laboratory calibration is the most accurate method to provide the full radiometric sensor calibration. The important tasks of vicarious calibration processes are to evaluate the validity of the laboratory calibration in flight conditions, to carry out the overall system validation and characterization and in general, to tune the image collection process (in particular the exposure settings); in some situations also to determine the absolute calibration. These are important steps to carry out especially after the sensor purchase and after updates and in beginning of the imaging season. As is the necessity in laboratory calibration, also in the vicarious radiometric calibration the fundamental prerequisite is to determine accurately the radiance entering the system. For this either radiative transfer calculations utilizing accurate information of atmospheric conditions and object reflectance (reflectance-based method), or simultaneous determination of the at-sensor radiance by a calibrated radiometer (radiance-based method) is used (see more details in **V**).

In the project, the empirical investigations were carried out using the photogrammetric systems DMC and ADS40 and a CASI hyperspectral scanner.

4.1 Characterization of the hyperspectral CASI system

The determination of the DMC radiometric calibration parameters was the main objective of the ICC's previous campaign in 2005 (Martinez and Arbiol, 2008). The obtained results were satisfactory enough, but the secondary objective concerning the results of atmospheric correction of DMC images was disappointing. Without field measurements the obtained values could not be applied. Even worse, the hypothesis that the CASI could be used as a calibration system was far from reality due to a poor knowledge on the detailed response of the hyperspectral sensor. With the 2008-campaign data it was possible to overcome the difficulties of the 2005-campaign (**I**, **II**).

The spectral shift characterization method of CASI is based on the hypothesis of global g-coefficients that need to be identically shifted for all the wavelengths for each look direction. The developed

methodology exploits the presence of the O2 atmospheric absorption band (about 760 nm) over a high reflectance cover in that wavelength. To determine the spectral shift, a non-orthorectified hyperspectral image over a vegetated area is aggregated in the along-track direction. This process generates a one-line image with 550 across-track spectral samples (look directions). Then, a subpixel Pearson correlation is computed for each one of the 550 spectra with a vegetation spectrum processed with the 6S code (Vermote et al., 1997) to take into account the effect of the O2 absorption band. The estimated spectral shift is then applied to the original image and the radiometric bands are spectrally resampled to fit the CASI channel nominal limits described by the g-coefficients. Details are given by Martínez et al. (**VIII**).

The first approximation of the spectral sensitivity of the bands was a rectangular response between the limits of each channel. This simple estimation works fine to correct the atmospheric scattering but is insufficient to solve the absorption regions. The manufacturer provided the accurate spectral sensitivities with a polynomial relationship between FWHM and wavelength, which showed values up to several times the nominal FWHM of the sensor (**VIII**).

Results by Martinez et al. (**VIII**) indicated that CASI smiling effect and accurate CASI spectral sensitivity had to be taken into account in order to obtain accurate atmospheric correction; in these circumstances correction yielded fewer artefacts on the atmospherically corrected spectra, even when only standard atmospheric parameters were used. The small artefacts still remaining around the absorption bands could be explained by a frequency dependence of the smiling effect, too week signal-to-noise ratio, etc.

4.2 Vicarious radiance based radiometric calibration of DMC in Banyoles

As an absolute radiometric calibration of the DMC was not available from the manufacturer during the empirical phase of the project, this relationship was obtained from simultaneous images from DMC and CASI sensors collected in the Banyoles campaign, by the radiance based calibration method. The CASI system is periodically recalibrated in the laboratory, and the idea was to transfer this calibration to the DMC. This is possible due to the fact that the acquisition geometry, atmospheric effects and illumination geometry are approximately equivalent for areas imaged simultaneously. Besides, the spectral resolution of CASI is high enough to reproduce DMC-like channels by integrating calibrated CASI hyper-spectral bands. In order to verify the previous hypothesis and because of the different FOV of DMC and CASI, only the central area of the DMC scenes were used. In addition, DMC pixels were aggregated to fit the coarse CASI spatial resolution. Then a median floating window filter was applied to both CASI and DMC imagery to avoid misregistration and other sources of noise. The radiometric calibration was performed through a linear regression between Digital Numbers (DN) from DMC and radiance values of a CASI image emulating DMC bands for each band and image (Martínez et al., 2007). Linear relationships with a zero intercept were found for all DMC used apertures and bands. All the R^2-values, characterizing the quality of least squares fit, were greater than 0.9. More results are given in **VIII**.

4.3 Vicarious reflectance based radiometric calibration of DMC in Sjökulla

The reflectance based vicarious calibration was applied to DMC using the Sjökulla images. The reflectance spectrums of several reference targets were measured during the campaign (Figure 2). The at-sensor radiances of the targets were calculated using the MODTRAN4 radiative transfer code. As in-situ measurements of atmospheric conditions were not available, the standard "Midlatitude summer" atmospheric settings and visibility information from the Helsinki airport in about 30 km

distance from the test field were used for the atmospheric radiative simulation. The images were collected using various exposure settings (aperture, exposure time), so the calibration was calculated using DNs that were normalized using the aperture and exposure time. Details of the approach are given by Markelin et al. in **VII**.

The results of the vicarious calibration showed that in general the sensor performance was linear; the R^2-values of linear regression were over 0.993 (Figure 4). The non-linear behavior with high at-sensor radiances is due to the saturation caused by failed exposure settings. In most cases the intercept and slope both were significant; absolute calibration parameters for different calculations are given in **VII**. Absolute radiometric laboratory calibration was not available for the DMC, so the vicarious and laboratory parameters could not be compared.

The vicarious calibration was calculated with nine different exposure settings (varying apertures and exposure times), and the radiometric stability of the system was assessed by evaluating the fit of the calibration parameters obtained for one setting with another setting, and for different days. The difference in R, G and B channels was on average 2.9–4.3% for the same day and the same aperture data, 3.5–4.5% for the same day and different aperture data and 3.1–5.2% for data collected on different days. The NIR channel showed weaker performance, and differences in corresponding cases were 5.7%, 9.2% and 10.9%, respectively. These differences appear in Figure 4 so that different lines are not accurately overlapping. Possible causes of these differences might be sensor instability, inaccuracy of the atmospheric modeling and inaccuracy of the reference values. The stability could be considered to be very good, as it derives from the instabilities of two independent sensors (PAN and MS). Detailed results are given in **VII**.

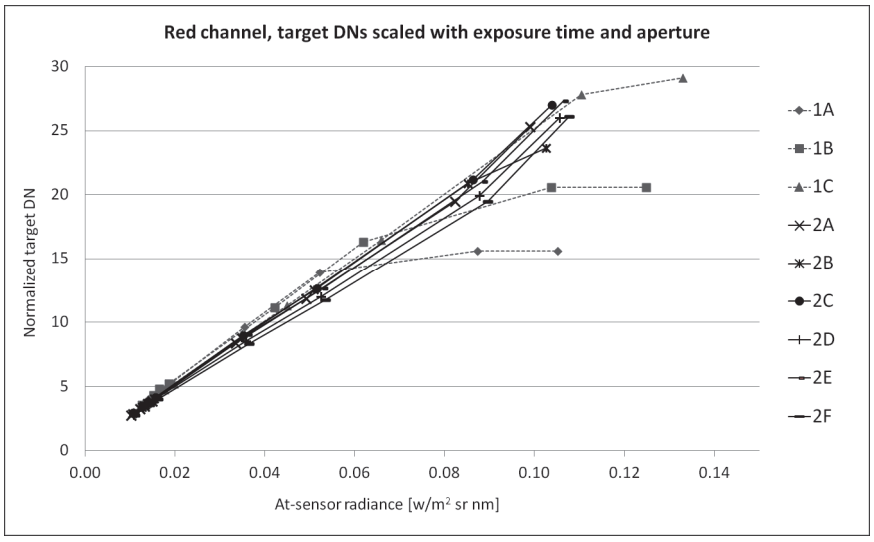

Figure 4. Normalized reference target average DNs as a function of simulated target at-sensor radiances. All settings, red channel. 1A-1C settings in 1 September, 2A-2F: settings in 25 September.

4.4 Vicarious reflectance based radiometric calibration of ADS40 in Hyytiälä

For the ADS40 campaigns in Hyytiälä the accurate in-situ measurements were available, including in-situ reflectance measurements of the reference targets and the atmospheric measurements of the

SMEAR-II and AERONET stations. An absolute radiometric calibration of the ADS40 was carried out using the reflectance based vicarious calibration method using ATCOR-4 (**XI**) and MODTRAN4 (**X**).

The main result from the reflectance based vicarious calibration was that both the gain and offset parameters were detected statistically significant (see detailed calibration parameters in **XXI**). Based on the laboratory calibration of the ADS40 (Beisl, 2006), only the gain parameter is needed. Differences in at-sensor radiances based on the MODTRAN4 based at-sensor radiance simulations by FGI and the ADS40 processing chain were larger than expected (10-20%) (Figure 5; **X**). Possible causes for the differences are on the one hand the inaccuracy of reference values and atmospheric modeling in the radiative transfer simulation, and on the other hand, possible inaccuracy of the ADS40 laboratory calibration. In this study it was not possible to find the exact reason for the differences. The assessment of accuracy of the reflectance images in Section 6.3 shows that using the vicarious calibration, the accuracy of ATCOR-4 based correction method improved significantly.

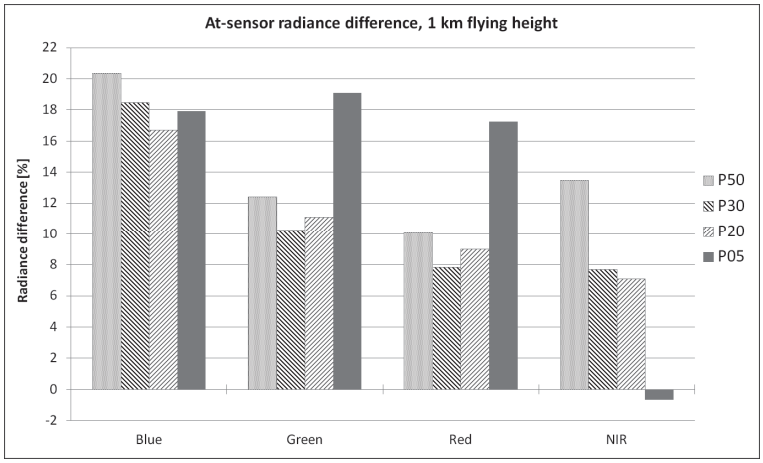

Figure 5. Relative differences of at-sensor radiances provided by MODTRAN4 and Leica XPro in different channels B, G, R and NIR on tarps on images from 1 km flying altitude. Difference = 100 * (MODTRAN4 – XPro) / XPro

5 Phase II – Spatial resolution assessment

The major factors influencing the image spatial resolution are the lens and detector properties. For high-quality photogrammetric sensors these are carefully designed and measured in laboratory. With multiple lens systems, such as DMC and UltraCam, the image stitching can cause additional deterioration of image quality. Important factors in dynamic applications influencing the image resolution are the forward image motion and the other motion components caused by the moving platform. Image quality is influenced also by the sensor exposure settings (Equation 2 and 3) and atmospheric conditions (Equation 1). The assessment of the system performance in flight conditions is important in two major situations: 1) to assess the performance of the entire imaging system and 2) to evaluate resolution of a specific campaign and individual images.

5.1 Methods for spatial resolution assessment

Spatial resolution measurements were performed for the Banyoles and Sjökulla DMC images. Different methods used in this study are described briefly below and summarized in Table 3 and 4.

Targets and participant	Method
ICC Siemens star, Banyoles, by ICC	The ICC method processes a region of interest that contains a single contour and makes a minimum square adjustment over the bi-dimensional function of the edge that is modelled as a sigmoid function. The five parameters are estimated in a least squares adjustment and the computed function is derived for obtaining the LSF (Line Spread Function). The FWHM (Full Width at Half Maximum) over the LSF is the measurement value (Talaya et al., 2008).
ICC Siemens star, Banyoles, IGN/MATIS	The IGN/MATIS used the Siemens star to determine the Modulation transfer functions (MTF) by evaluating contrasts of bright and dark sectors (**XVI)**.
Entire image, Banyoles, by IGN/MATIS	IGN/MATIS used a method that measured the local image sharpness over the entire image by using Haar Wavelets Transform (**XVI)**.
FGI RP targets, Sjökulla, by FGI	RP-values were automatically determined from line bar targets by finding the narrowest detectable lines (Honkavaara et al. 2006; Honkavaara, 2008).
FGI Siemens star, Sjökulla, by FGI	PSF-values were determined from Siemens star by first estimating the MTF based on contrasts of adjacent sectors and then calculating the PSF (Honkavaara et al., 2006; Honkavaara 2008)

Table 4. Methods for spatial resolution assessment.

The conventional, accurate method for spatial resolution measurement is to use artificial targets, such as line bar target, Siemens star or edge target:

- In the Banyoles campaign (Figure 1), there was a Siemens star made of canvas of size of 100 m^2 and with 5° sectors; the target appeared in different positions on 9 DMC images from the flying height of 820 m, with a GSD of about 8 cm.

- In the Sjökulla campaign (Figure 2), a Siemens star and resolving power (RP) line bar targets were available. The FGI's Siemens star is a semicircle with a size of 72 m^2 (radius of 6.8 m and 10° sectors). In the line bar targets, the widths of lines are 3-12 cm. In the image blocks, the resolution targets were located over the image area on 35 positions on first acquisition day and on 18 positions on second acquisition day. GSD was 5 cm and flying height was 500 m.

The methods that can evaluate image resolution automatically using the campaign image data and do not require artificial targets are very attractive. This type of a method has been developed by IGN/MATIS. The image sharpness map is determined by the Haar Wavelets (Brédif and Lelégard, **XVI**).

Influences of the following factors were studied in the resolution evaluations

1. Resolution in different positions in the image (all participants)

2. Resolution in radial and tangential directions (IGN/MATIS)

3. Resolution in flying direction and cross-flight direction (FGI)

4. Influence of exposure time and aperture (FGI)

5. Influence of atmosphere (ICC)

5.2 Results of spatial resolution assessment of the imaging system

The ICC used the Siemens star to determine the PSF. The averaged resolution obtained for each image did not show the expected correlation between the distance to the center of the image and the resolution. These unexpected results are probably due to variables of the acquisition process not taken into account during the study.

The analysis of MTF by IGN/MATIS from Siemens star showed that the optical system was isotropic and the lens was compatible with the CCD-array (no aliasing). The resolution was better in a centered band parallel to the flight direction. The sharpness map based on Haar wavelets derived from 156 images is shown in Figure 6. It shows some possible defects due to image formation process based on mosaicking four images and some additional minor defects. The method is a potential tool for detection of optical defects and the qualification of the mosaicking of multiple sensor images into a larger composite image. The conclusion of the IGN/MATIS evaluations was that the panchromatic photos provided by the DMC camera did not present major faults. Detailed results are given by Brédif and Lelégard (**XVI)**.

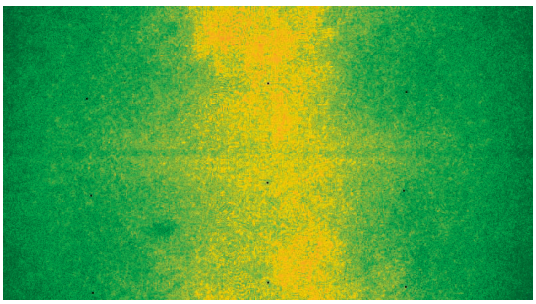

Figure 6. Image sharpness map obtained using 156 images of the Banyoles DMC campaign by IGN/MATIS (XVI). Yellow indicates better and green worse image sharpness.

The RP measured using the Sjökulla image data is shown as function of distance from image center in flight and cross-flight direction in Figure 7. Resolution was dependent on the distance from the image center: the farther the target was from the center, the worse the resolution was. By using linear regression, the resolution was worse by a factor of 1.5 in the furthest image corner compared with the image center. The same phenomenon had already been demonstrated both theoretically and empirically by Honkavaara et al. (2006). The theoretical expectation regarding the resolution of an image with a 12 µm pixel size is 84 lines/mm; with the tilted DMC images the theoretical expectation regarding the decrease of resolution is up to 1.6 in the image corner. The resolution was slightly better in the cross-flight than in the flight direction, which is most likely caused by the forward image motion. Any significant influences of the exposure settings (f-stop: 8, 11; exposure time 3.5–6.5 ms) on the resolution could not be detected. The evaluations of MTFs provided similar conclusions.

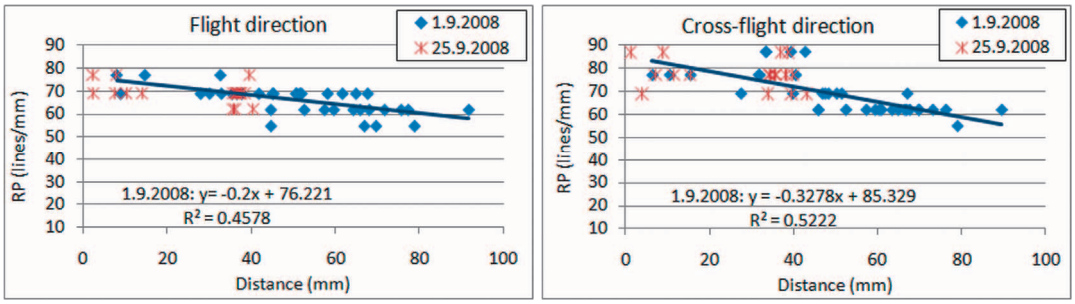

Figure 7. Resolving power as the function of the radial distance from the image center on flight (left) and cross-flight (right) directions.

5.3 Simulations on influences of atmosphere on spatial resolution

Imaging systems suffer from resolution degradation due to both the optical system and the atmosphere. Therefore, real resolution of the image is different from purely geometrical pixel size and the Ground Sampling Distance (GSD). The ICC analysed the image resolution as a function of the atmospheric radiative conditions. The 6S (Vermote et al., 1997) code was used to model the atmosphere. Atmosphere type, aerosol model and total load, illumination and observation geometries and spectral range were taken into account when computing simulations. The results were also compared with the resolution measures on the real images taken with the DMC images from Banyoles. See details in **IX.**

The histogram of the resolution (FWHM of LSF in pixel units) after implementing a step-like weather simulation for panchromatic channel showed a skewed distribution of resolution values with a large tail towards lower values of resolution (FWHM greater) (Figure 8). This distribution indicates that in the majority of cases the resolution is about the maximum frequency, but there are a lot of cases where the atmosphere will produce a large loss of resolution. Besides, there is a high dependence on wavelength, and the maximum effect appears at lower wavelengths. These simulation results and the resolution measured in the real DMC panchromatic images are compatible. A more detailed analysis shows that the type and amount of aerosols influence the loss of resolution (Figure 9). Details are given in **IX**.

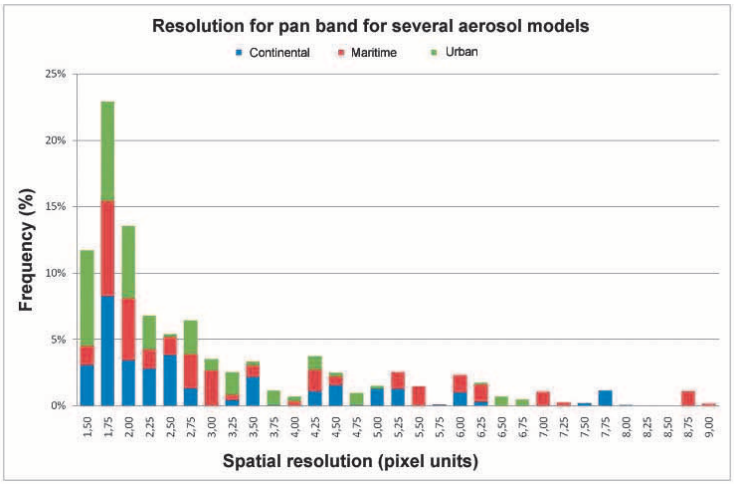

Figure 8. Resolution for DMC pan band with several aerosol models applied (FWHM of LSF in pixel units). (IX)

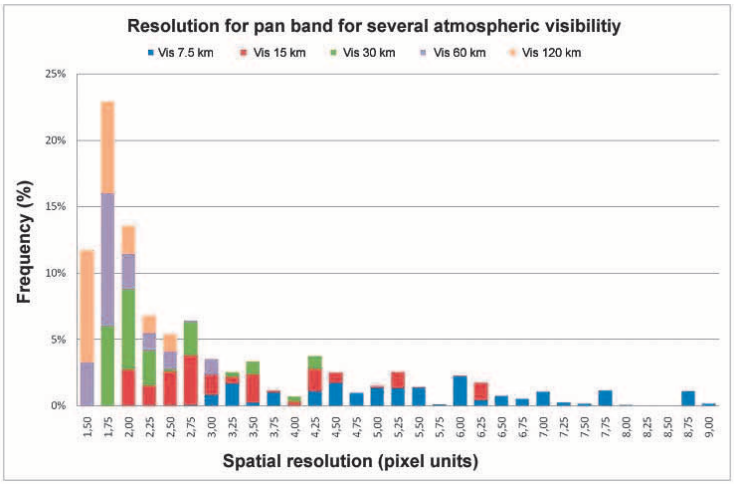

Figure 9. Resolution for DMC pan band with varying atmospheric visibility (FWHM of LSF in pixel units). (IX)

6 Phase II – Reflectance image production and image block equalization

The desired output products from the radiometric processing are reflectance images, true color images and in general, balanced image data. The radiometric processing method should take into account influences caused by the sensor, atmosphere and objects. The most significant sensor related influences are the sensor spectral and radiometric response, sensor instability and sensor settings during the data collection (Equation 2 and 3). The atmosphere has great influences on the image radiometry. The most significant factors to be compensated are the atmospheric path radiance and the influences of diffuse light (Equation 4). Finally with the large-format photogrammetric cameras the BRDF-effects have to be accounted for (Equation 5).

6.1 Methods for reflectance image production and image block equalization

Several relevant approaches for reflectance image calculation and image block equalization were evaluated in the project. These included the Pepita radiometric block adjustment method of IGN, two commercially available correction methods based on radiative transfer calculations (ReSe ATCOR-4 and Leica Geosystems XPro) and an empirical line based method (Table 3).

6.1.1 Pepita of IGN

The "radiometric aerial triangulation" Pepita software is a method for equalising a block of digital aerial images, which can be considered as relative radiometric calibration (Chandelier and Martinoty, 2009; **XVII**). It is based on a parametric, semi-empirical radiometric model taking into account BRDF, haze differences between blocks of images, solar elevation, sensor settings (exposure) and a optional radial component (mainly for chromatic aberration). The model parameters are computed through a global least-squares minimization process, using radiometric tie points in overlapping areas between the images. As a result, a relative equalization between the images is obtained. The method has been used in the IGN orthoimage workflow since 2005. At the beginning, Pepita has only been tested and used on IGN-v1 camera images, giving satisfying results. In 2008, some tests were carried out on DMC images, but the results did not meet the requirements of the IGN orthoimage database specifications. In 2009, IGN acquired its own UltraCam XP camera and Pepita is currently used both on UXP and IGN-v2 cameras.

6.1.2 ATCOR-4 of ReSe

The ATCOR-4 performs a physically based atmospheric and topographic correction for airborne scanner data in the solar (0.35-2.55 μm) and thermal (8-14 μm) spectral regions. The correction is based on pre-calculated MODTRAN® look-up tables of the atmospheric radiation field (Richter and Schläpfer, 2002; Richter and Schläpfer, 2011; **XXII**). The output in the solar region is the surface reflectance and in the thermal region it is the surface (brightness) temperature and emissivity. The capabilities of the software include determination of the aerosol map (requires bands in the near infrared and/or in the short wave infrared region) and the spatial water vapor map (requires bands in the 940/1130 nm region), haze and cirrus cloud removal (low altitude haze) and inflight sensor calibration using ground reference targets. ATCOR-4 is for wide FOV airborne scanner imagery and for all terrain types, and it includes the capability for radiometric correction in rugged terrain with cast shadow, topographic and BRDF corrections. The basic assumption of ATCOR-4 is a stable, accurately calibrated sensor.

6.1.3 XPro of Leica Geosystems

Leica Geosystems XPro software takes care of the entire post-processing workflow of the ADS-imagery from data download to the generation of stereo models and orthoimages. Main features from the radiometric point of view are the options to produce ground radiance and ground reflectance images. The default product of XPro is calibrated DN, which relates the pixel data to at-sensor radiances. There are two options to produce ground radiance data: the Dark Pixel Subtraction and the Modified Chavez methods. Ground radiances are still dependent on the illumination level and vary from flight line to flight line. Ground reflectances are calculated by dividing the reflected radiance by the incoming solar irradiance, which is estimated based on the radiative transfer equation by Fraser et al. (1992) and using a parameterization of the atmospheric parameters based on the method of Song et al. (2003). All three correction methods are based on an automatic dark object method to tune the corrections to the actual atmospheric conditions. Additionally, BRDF correction based on a modified Walthall model is implemented in XPro. All corrections rely entirely on a priori calibration information and parameters derived from the image data. The details of the correction methods are given by Beisl et al. (2008) and the method was analysed by Heikkinen et al. (**XII**).

6.1.4 Modified empirical line method

Empirical line method is widely used in reflectance calibration of remote sensing image data (Smith and Milton, 1999). In the method, a linear relationship of the DNs and ground reflectances is determined. In this study a modified version that takes into account the anisotropy of the reference target and uses DNs that are normalized with respect to size of aperture and exposure time was used. Details of the approach are given by Honkavaara et al. in **VI**.

6.1.5 Performance assessment of radiometric correction methods

The performance assessment of radiometric correction is dependent on the type of correction performed.

The validation of reflectance images can be carried out using reflectance reference measurements. In this investigation, artificial reference targets installed in the area and surfaces existing in the object were used as reference (see Section 3.1); in each reference target ground truth measurements were carried out using spectroradiometers. In most cases the nadir reflectances were measured, but in the case of FGI reference measurements also BRFs were measured in many cases. Repeatability of the reflectance image generation was evaluated by comparing images collected in repeated acquisitions of same targets from the same or different flying heights.

The difference of the reflectance in image and the reference reflectance is calculated for each target to obtain the reflectance error in reflectance units:

$$E_{refl} = \rho_{data} - \rho_{ref} \tag{6}$$

This difference is divided by the reference and multiplied by 100 to get the reflectance error in percents:

$$E_{refl\%} = 100(\rho_{data} - \rho_{ref}) / \rho_{ref} \tag{7}$$

From 6 and 7, root mean square error values ($RMSE_{refl}$ and $RMSE_{refl\%}$) are calculated for each image and sensor channel. The $RMSE_{refl\%}$ is:

$$RMSE_{refl\%} = \sqrt{(\sum E_{refl\%}{}^2)/n} \tag{8}$$

where n is the number of reference targets used.

Quantitative evaluation methods were not available for relative radiometric correction methods. The radiometric differences between images were visually estimated and the residuals at radiometric tie points were considered. Quantitative criteria for equalization methods could be based on radiometric differences between tie points before and after correction.

6.2 Results of radiometric block adjustment by Pepita software

The Pepita software was used to correct the DMC Banyoles image materials. The following conclusions were drawn by Chandelier (**XVII**) based on the results. The solar elevation, exposure time and aperture values were well corrected. The BRDF model worked well especially on forest and agricultural parcels. As expected, the BRDF model did not fit on the lake. In urban areas, the effect of the equalization was less visible: highest residuals are observed confirming that tie points are not really homogeneous (a DSM should be used). High residuals occurred also in the lake. The radial component didn't improve significantly the equalization: on the contrary, in urban areas, the radiometric model may not be convergent causing bad equalization for several images. As a conclusion, Pepita could be used as a tool for relative radiometric calibration for DMC images. To ensure that this result is correct, further testing should be done with additional datasets (more images, different dates…). Further improvement for the method would be a mode for absolute radiometric correction to calculate reflectance images. Performance of Pepita is fully automatic and it fulfills all the operational requirements of the IGN. Detailed evaluation is given by Chandelier in **XVII**.

6.3 Reflectance image generation using methods based on atmospheric radiative simulations

Reflectance calibration of the Hyytiälä data was carried out by several approaches (Table 5). FGI and Swisstopo used XPro to produce atmospherically corrected (ATM) images and ATM with BRDF correction. ReSe performed ATCOR-4 processing using Leica's calibration parameters and in-flight calibration parameters based on reference targets P05 and P50; cast shadow correction was tested in the latter case. The FGI carried out ATCOR-4 processing using Leica's laboratory calibration and in-flight calibration parameters derived separately for each image and also one set of calibration parameters derived from the 1 km flying height image and used for all images. Details of these evaluations are given in **XI** and **XXII**.

Different objects were evaluated separately:

- Artificial black tarp (P05 with reflectance 0.057 on ADS40 green channel)
- Artificial bright tarps (P20, P30 and P50 with reflectance 0.181, 0.261, 0.442)
- Uniform object surfaces (asphalt, gravel, sand)
- Grass surfaces

	XA1	XA2	XF1	XF2	AL1	AL2	AL3	AV1	AV2	AV3	AV4	AV5
Participant	FGI	ST	FGI	ST	FGI	FGI	ReSe	FGI	FGI	FGI	ReSe	ReSe
Cal.	lab	lab	lab	lab	lab	lab	lab	vic.	vic.	vic.	vic.	vic.
Atm.	imag.	imag.	imag.	imag.	in-situ	imag.	imag.	in-situ	imag.	imag.	imag.	imag.
Other			BRDF	BRDF						cal.1B		shd.

Table 5. Processing parameters of all evaluated image versions (X for XPro, A for ATCOR-4). Cal.: origin of the sensor radiometric calibration (lab: laboratory, vic: vicarious in-flight radiometric calibration with tarps P05 and P50); Atm.: origin of the atmospheric parameters used (imag.: derived from the imagery, in-situ: in-situ measurements). Other: BRDF = with empirical BRDF-correction, cal.1B = sensor calibration based on image line 1B and four tarps; shd. = with cast shadow correction.

Figure 10 gives the reflectance accuracy evaluation results of different methods for an image strip collected from 2 km flying height on good atmospheric conditions (difference to reference value in % of the reflectance) for bright tarps. On the bright tarps, when in-flight calibration parameters were used (ATCOR-4 processing, image versions AV1-AV5), the differences were well below 5% (with a minor exception). If laboratory calibration parameters were used (XPro image versions XA1 and XA2, ATCOR-4 image versions AL1-AL3), the differences were clearly higher in blue and NIR channels (7-13%). The accuracy was the best in the case where in-flight calibration parameters from 1 km flying height were used (dark target: better than 5%, bright targets: better than 1.5%). On the black tarp, when Leica's laboratory calibration was used, differences were 5-30%, depending on the channel; with in-flight calibration the differences were again lower than 5%. When cast shadow correction option of ATCOR-4 was used, large differences (60-120%) appeared on black target; obviously shadow correction has considered black target as a shadow.

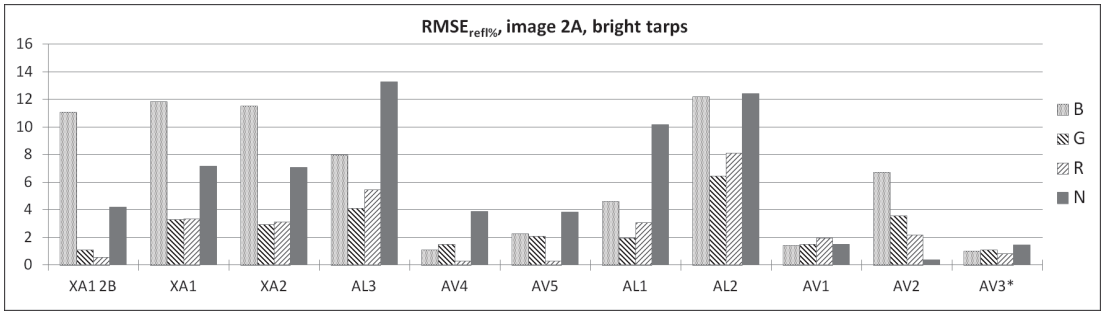

Figure 10. RMSE for reflectance differences (in %) all methods, 2 km flying height (nadir looking image line 2A and backward looking image line 2B for XA1), bright tarps.

The results of XPro correction of all flying heights indicated that for the evaluated challenging data set, up to 5% reflectance accuracy could be obtained with uniform targets. The accuracy was influenced by the flying altitude (1-4 km), channel (R, G, B, NIR), level of cloudiness and target properties. With the XPro there appeared a clear dependency of the reflectance error to the magnitude of reflectance - both in reflectance units and in percents. (**XI**)

An analysis of theoretical basis of XPro by Heikkinen et al. (**XXII**) showed that the correction is based on planar surfaces and that the highest quality reflectance calibration was possible only in sun

illuminated areas. The BRDF correction method is best suited for applications where visually uniform mosaics are of interest.

These results are very promising. The evaluations showed that a reflectance accuracy level of 5 % is possible with sensor laboratory calibration and without any reference measurements. With vicarious radiometric in-flight calibration of the sensor, reflectance accuracies even better than 5 % were achieved. Issue with very dark targets is that a small error in atmospheric correction leads to large relative error, so larger errors are expected with dark objects. With natural targets (grass, forest trees) the non-homogeneity of objects will cause deviations in all comparisons. The results suggested that the laboratory calibrated values might not be accurate enough especially on NIR channel, but also errors in ground truth reflectance values or in atmospheric modeling can cause similar effects. The poorer results in blue channel can be caused by larger atmospheric influences. These issues need to be studied further. The full comparative results of all data sets (including also data from cloudy conditions) and processing methods are presented in **XI** and **XXI**.

Swisstopo evaluated the XPro 4.2 and ReSe evaluated the ATCOR-4 from the productivity perspective. XPro fulfilled the productivity requirements of Swisstopo (**XV**). The evaluation of ATCOR-4 by ReSe showed that the further tuning of software is necessary to fulfil all efficiency and usability requirements of NMAs (**XXII**).

6.4 Reflectance image generation using empirical line method

An empirical line based radiometric correction was carried out with the Sjökulla image block. Dark and bright targets were used as reference, and the reflectance values measured in laboratory were used. The major objective was to calculate BRFs from the photogrammetric image block. A comparison of BRF of black gravel measured in laboratory and from DMC images is shown in Figure 11. In the reference targets, the reflectance RMSEs were 3-7%; some deterioration in accuracy might be due to the fact that reflectance values determined in laboratory were used, instead of in-situ values. The results show that the photogrammetric image block can be used indeed for providing BRFs, but the atmospheric correction is critical. Furthermore, in the case of vertical images, range of observation angles is dependent on the field of view of the sensor; observation angles are smaller than ±40º with the DMC. The empirical line based approach does not fulfil productivity requirements of NMAs, because it requires reflectance targets in object areas. However, the method is functional in small area remote sensing applications.

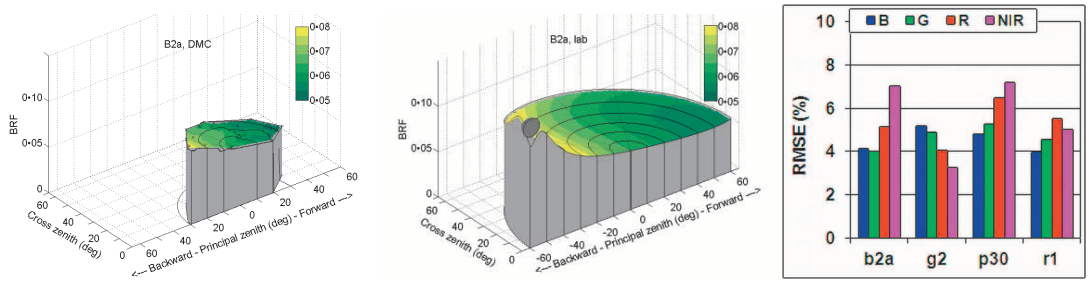

Figure 11. 3D-BRF plot of black gravel measured by the DMC (left) and at laboratory using goniospectrometer (center) and RMSEs on all evaluated images for different check targets (right). (VI)

7 Phase II – Application oriented investigations

Some application oriented investigations were carried out in the context of the project. Comprehensive investigations on tree species classification were carried out using the ADS40 image data sets collected in Hyytiälä by Heikkinen et al. **XII** and Korpela et al. **XIII**. The NDVI orthophoto layer of Catalonia is given as an example of a new possibility of the novel technology (Martinez et al., **XIV**).

7.1 Tree species classification with ADS40 data

The suitability of the ADS40 at-sensor radiance, reflectance and BRDF-corrected reflectance images created by the XPro software on single tree level species classification was studied by Heikkinen et al. (**XII**) and Korpela et al. (**XIII**). They developed a method in which the crown level illumination and occlusion conditions were determined. The method is based on modelling the crown shapes and visibility/shading conditions by using dense LiDAR data. Based on the data, the reflectance characteristics of tree species (within tree species variation, reflectance anisotropy, proximity effects, etc.) were studied in sun illuminated and shadowed conditions. The data with known illumination conditions were then used in further classification experiments by quadratic discriminant analysis by Korpela et al (**XIII**) and support vector machine classification by Heikkinen et al. (**XII)**.

Evaluations of reflectances of different versions of ADS40 images indicated that in general, reflectance variations within species in the same illumination class were high (the coefficient of variation was 13-31%) (**XIII**). Results on reflectance anisotropy showed that if BRDF correction was not applied, a clear brightening towards backward scattering direction appeared. This is an expected behavior, because in this case the sensor is observing the non shaded parts of trees, opposed to the situation in the forward scattering direction, where the shadowed parts are observed. The simple BRDF correction approach of XPro compensated efficiently the BRDF effects, but did not improve the classification results.

Classification experiments with reflectance images provided a total accuracy of about 75-79% with single ADS40 view and 78-82% with two ADS40 views (Heikkinen et al., **XII**). In some cases (the training and classification data from different flight lines) the use of reflectance images provided better classification results than the at-sensor radiance data. One limitation of the study was that the images were collected in the end of August, and this data might not be optimal for tree species separation.

7.2 NDVI data sets generation from DMC images

The good results obtained with DMC encouraged ICC to develop a NDVI orthophoto map layer of Catalonia (more than 32,000 km²) during 2011 (Figure 12) (Martinez et al., **XIV**). It consists of the Normalized Difference Vegetation Index (NDVI), which provides a measure of vegetation density and condition. It is influenced by the fractional cover of the ground by vegetation, the vegetation density and its greenness. It indicates the photosynthetic capacity of the land surface cover.

The phases of the NDVI orthophoto layer generation are the transformation of the DNs to at-sensor radiances using the laboratory radiometric calibration information of the DMC, calculation of reflec-

tance images and finally NDVI image calculation from the red and infrared reflectances. In this first implementation the at-sensor reflectance values are used; the atmospheric correction is not applied. First user of this layer will be the Agriculture Department of the Generalitat de Catalunya (regional government) just a few weeks after the flight. Next, a few months later the data will be published. Then, the vegetation layer is provided as a web map service (WMS) Geoservice and is disseminated according to ICC data policy.

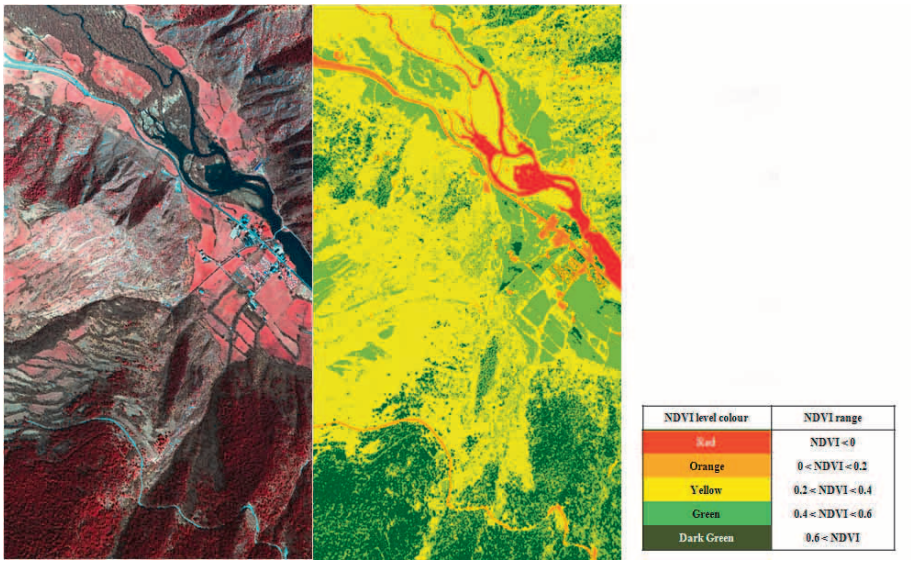

Figure 12. DMC CIR image (left) and at-sensor NDVI image (right). (Martinez et al., XIV)

8 Summary and discussion

8.1 Major conclusions of the EuroSDR project

The EuroSDR project "Radiometric aspects of digital photogrammetric airborne images" was carried out in 2008-2011. The two phases of the project were a review and empirical investigations. The project participants represented stakeholder groups from NMAs, software development and research.

The review phase consisted of a review to the theoretical background and a questionnaire on current status of the radiometric processing of photogrammetric image data. The results showed that the radiometric processing of photogrammetric sensors was inadequately managed. The high-quality sensors could give much higher performance potential, if radiometry was more rigorously processed.

Image blocks for the empirical investigation were collected by Leica Geosystems ADS40 in Finland and by Intergraph DMC in Spain and Finland. Unfortunately data from UltraCam-system was not available in the empirical investigation.

The empirical investigations were carried out on four major topics:

1. Vicarious radiometric calibration and characterization
2. Spatial resolution assessment
3. Radiometric correction of image blocks.
4. Application oriented studies.

The major emphasis in the study was the physical reconstruction of the radiometry of the imaging event, which is a mandatory step in automated, radiometrically quantitative data processing. In principle, the procedure is similar to the approaches that have been used in satellite based remote sensing and in processing of spectroradiometric image data for decades. However, the photogrammetric environment provides some new challenges for the processing. These include extremely high spatial resolution, stereoscopy, strong image block structure, huge volume of collected data and the fact that the imagery are collected in more variable atmospheric and illumination conditions, with horizontal visibilities varying typically between 15 – 50 km and very low solar elevations of 20º and even less.

The vicarious radiometric sensor calibration was the most favorable with the Banyoles campaign data because of the rigorous project set up and excellent weather conditions. The problem in the Hyytiälä campaign was the slightly unfavorable weather conditions and in the Sjökulla campaign the missing in-situ AOT measurements. Results showed that the vicarious radiometric calibration and validation was necessary. The analysis of radiometric calibration values of ADS40 indicated that the laboratory calibration was not compatible enough with the physically based atmospheric correction method ATCOR4. In the case of the hyperspectral sensor CASI, the spectral smile effect needed to be determined in flight conditions.

Spatial resolution analysis included resolution measurements using artificial targets as well as image sharpness measurement based on image data. Further evaluations included assessment of influences of exposure time, aperture and atmospheric conditions in resolution. The results showed that the resolution of DMC images was good and fulfilled theoretical expectations. Important aspects in the study were the novel Haar wavelet based approach for the estimation of the local image sharpness, which could be used to detect faults in the sensor, based on the information in images. This approach has a great value from the operational point of view. All the participants used different methods and indicators in the assessment of spatial resolution; to make results more comparable standardization of methods and indicators are needed.

There are already approaches for reflectance image calculation and radiometric equalization of photogrammetric image data that are suited for production environments. Especially, IGN's Pepita software and the XPro software fulfil the productivity requirements. At best, the accuracy of reflectance images by XPro was up to 5% without any ground reference targets. Improvements are still needed for the approaches. For many software products the processing of a whole photogrammetric block is still a limitation. Improvements are also needed in processing of shadowed regions and in treatment of object reflectance anisotropy. Finally, accurate absolute sensor calibration is needed to allow physically based radiometric processing methods.

Application oriented studies covered two aspects: tree species classification and novel NDVI data products based on national photogrammetric image data. Results showed that accurate radiometric correction is advantageous for the applications. It is important to consider the applications when developing methods for radiometric correction, and on the other hand, the applications (e.g. automatic classification methods) should take into account the level of radiometric correction of the input data. The evaluated applications are not the most urgent issues form the points of view of NMAs, but clearly indicated that the imagery have a lot of potential in new application areas. Further studies should consider the impacts of radiometric correction in applications of NMAs.

The fundamental objectives of the investigation are presented in Section 1.1. These objectives were fulfilled as follows:

1. Knowledge of radiometric aspects was improved by the means of articles, presentations in international conferences, special radiometry sessions in European Calibration and Orientation Workshops (EuroCOW) 2010 and 2012 and an EudoSDR Eduserv course „Radiometric performance of Digital Photogrammetric Cameras and Laser Scanners" organized in co-operation with Vienna University in spring 2012.

2. The existing methods and procedures for radiometric image processing were studied from quality and productivity perspectives.

3. The comparison of operative solutions using same test data set was realized comprehensively only with the ADS40 data from Hyytiälä, because general solutions for radiometric correction were available only for pushbroom type sensors. On the other hand, analysis was made from many different points of views that all are relevant for NMAs; this can be seen as very valuable approach because the technology is not yet mature.

4. The application oriented investigations showed some advantages of the rigorous radiometric calibration and correction in automated processing. Operational applications are still mostly interactive, and for these applications the rigorous radiometric processing does not provide so clear advantages. The correction approaches and interpretation methods should be further improved in order to obtain full advantage of the high-quality radiometry.

8.2 Recent developments

Since the beginning of the project, improvements were achieved in the processing of the airborne image data.

When the project started in 2008, the ADS was the only photogrammetric sensor for which absolute radiometric laboratory calibration was available (Beisl, 2006). Since 2009, a high-accuracy calibration is offered also for the frame sensor DMC (Ryan and Pagnutti, 2009). Absolute calibration methods have not been presented for other photogrammetric cameras.

In 2008, commercial software for the rigorous, physically based reflectance image generation was available only for the pushbroom scanner based images. For pushbroom scanners, physically based, rigorous atmospheric correction methods have been available for decades, because traditional airborne and spaceborne hyper- and multispectral scanners are based on this principle. Leica Geosystems has offered a high performance radiometric correction for the ADS already since 2008 (Beisl et al., 2008), and this software was evaluated in this study. The method showed a great potential, but also many improvement ideas were identified. A new ADS-sensor based version of the ATCOR-4 software is now under development by ReSe for the processing needs of the Swisstopo (Schläpfer et al., 2012). Important improvements of the software are the better usability and shadow correction optimized for high resolution imagery. These aspects are relevant for NMAs, and especially in Switzerland and in general in areas with large topographic differences.

Rigorous radiometric processing methods are becoming available for frame sensor images, too. With these sensors the radiometric block adjustment is a central part of the algorithm. During the review phase in 2008, the Pepita software of the IGN was undoubtedly the most advanced method for the correction of frame image blocks, applying the atmospheric parameters and BRDF correction (Chandelier and Martinoty, 2009). Now, similar approach has been recently implemented also to the UltraMap processing software of the UltraCamXp (UltraCam, 2012). Recently, several new approaches for BRDF correction and atmospheric compensation have been presented in scientific literature (Collings et al., 2011; López et al., 2011).

The use of airborne photogrammetric images in automation of various mapping tasks is still quite limited, and in the application related studies the level of radiometric processing is rarely considered.

International standards for airborne imaging systems are evolving, but slowly. For satellite sensors there already exists an international test field network (Chander et al., 2007). For airborne sensors, Cramer et al. (2010) recently presented a test site concept. A review of methods and test sites for assessment of spatial resolution of EO data products was presented by Pagnutti et al. (2010).

8.3 Recommendations and suggestions for the future developments and investigations

As the final conclusions we give the following recommendations and suggestions

1. The knowledge about the possibilities of the new sensors should be still improved, especially for those who produce and utilize (large-format) photogrammetric images.

2. Standardization of radiometric terminology and processing methods is needed. In particular this is to help users that purchase data from different data providers and for image fusion in general.

3. Radiometric processing methods should be improved further. Important topics for future developments include radiometric calibration of sensors, image block processing, shadow and BRDF correction, and management of image data blocks collected in different atmospheric conditions, multiple times and using different sensors.

4. Rigorous, physically based radiometric correction should be a basic procedure in photogrammetric processing chains and it is expected that it will simplify greatly subsequent data processing needs and interpretation processes of NMAs.

5. Accurate (quantitative) interpretation methods that utilize accurate image radiometry should be developed. Powerful new approaches could be based on reflectance images, laser scanning data and image matching based DSMs.

6. Possibilities for new data products should be considered. The new NDVI data product of ICC is an example of these possibilities.

7. Radiometric calibration and validation of entire data processing chain in test field was shown to be important. Permanent test fields were proven to be powerful tools for these processes. Availability of permanent targets and permanent measurement equipment will simplify greatly the in-situ measurement efforts required in campaigns; without permanent tools the calibration/validation campaigns are very laborious and there is a great risk that they will fail.

8. Not all important radiometry related topics were covered in this investigation. Uncovered topics include operational quality control methods for production processes, pansharpening, image enhancement and colorimetric calibration. Also, the applications and advantages of rigorous radiometric correction were only scratched.

9 Conclusions

We presented the results of the EuroSDR project "Radiometric aspects of digital photogrammetric images" in this report.

The new sensors and processing methods showed excellent radiometric potential. We expect that the high resolution, geometrically and radiometrically accurate, multi-spectral, stereoscopic photogrammetric imagery could provide new possibilities for remote sensing applications. The Internet-based orthophoto and environmental model servers have an important role in providing up-to-date information for large public audiences. These nationwide databases could also be one component of a more general Earth analysis process, integrated with spaceborne images, hyper-spectral images, laser point clouds and terrestrial data, and all other types of geospatial information. Investigation, development and co-operation are needed in this area in order to further standardize the processes.

Acknowledgements

Our sincere acknowledgements go to all the project participants for the fluent and innovative co-operation. Without their support this project would not have been possible.

References

Beisl, U., 2006. Absolute spectroradiometric calibration of the ADS40 Sensor. In: The International Archives of the Photogrammetry, Remote Sensing and Spatial Information Sciences, Paris, France, Vol. XXXVI, part 2.

Beisl, U., Telaar, J., and Schönermark, M. V., 2008. Atmospheric correction, reflectance calibration and BRDF correction for ADS40 image data. In: The International Archives of the Photogrammetry, Remote Sensing and Spatial Information Sciences, Beijing, China, Vol. XXXVII, part B7.

Chandelier, L., Martinoty, G., 2009. Radiometric aerial triangulation for the equalization of digital aerial images and orthoimages. Photogrammetric Engineering & Remote Sensing 2009, 75, 193-200.

Chander, G., Christopherson, J.B., Stensaas, G.L., Teillet, P.M., 2007. Online catalogue of world-wide test sites for the post-launch characterization and calibration of optical sensors. In Proceedings of IAC International Symposium, Hyderabad, India, 2007.

Collings, S., Cacetta, P., Campbell, N., Wu, X. 2011. Empirical models for radiometric calibration of digital aerial frame mosaics. - IEEE Transactions on Geoscience and Remote Sensing 49 (7): 2573-2588.

Cramer, M., Grenzdörffer, G. and Honkavaara, E., 2010. In situ digital airborne camera validation and certification -The future standard? International Archives of the Photogrammetry, Remote Sensing and Spatial Information Sciences, 38(B1), 7 pages.

Fraser, R. S., Ferrare, R. A., Kaufman, Y. J., Markham, B. L., and Mattoo, S., 1992. Algorithm for atmospheric corrections of aircraft and satellite imagery. International Journal of Remote Sensing, 13(3), pp. 541-557.

Hari, P., Kulmala, M., 2005. Station for Measuring Ecosystem-Atmosphere Relations (SMEAR II). Boreal Enviroment Research 10(5), pp. 315-322.

Holben, B.N., Eck, T.F., Slutsker, I., Tanré, D., Buis, J. P., Setzer, A., Vermote, E., Reagan, J.A., Kaufman, Y.J., Nakajima, T., Lavenu, F., Jankowiak, I., and Smirnov, A., 1998. AERONET—A federated instrument network and data archive for aerosol characterization. Remote Sensing of Environment 66(1), pp. 1–16.

Honkavaara, E., Jaakkola, J., Markelin, L., and Becker, S., 2006. Evaluation of resolving power and MTF of DMC. International Archives of Photogrammetry, Remote Sensing and Spatial Information Sciences, 36(A1), 6 pages.

Honkavaara, E., 2008. Calibrating digital photogrammetric airborne imaging systems using a test field. Doctoral thesis. Publications of the Finnish Geodetic Institute, N:o 140, Kirkkonummi, Finland, 2008.

López, D.H., García, B.F., Piqueras, J.G., Aöcázar, G.V., 2011. An approach to the radiometric aerotriangulation of photogrammetric images. ISPRS Journal of Photogrammetry and Remote Sensing 66 (2011): 883-893.

Martínez, L., Arbiol R., 2008. ICC experiences on DMC radiometric calibration. International Calibration and Orientation Workshop EuroCOW 2008. Castelldefels (Barcelona), 30 Jan-1 Feb.

Martínez, L., Palà, V., Arbiol, R., Pérez, F., 2007. Digital Metric Camera radiometric and colorimetric calibration with simultaneous CASI imagery to a CIE Standard Observer based color space. IEEE International Geoscience and Remote Sensing Symposium. Barcelona, 23-27th July.

Pagnutti, M., Blonski, S., Cramer, M., Helder, D., Holekamp, K., Honkavaara, E., Ryan, R., 2010. Targets, Methods and Sites for Assessing the In-Flight Spatial Resolution of EO Data Products. Canadian Journal of Remote Sensing, Vol. 36, No. 5, pp. 583–601, 2010.

Richter, R., and Schläpfer, D., 2002. Geo-atmospheric processing of airborne imaging spectrometry data. Part 2: atmospheric/topographic correction", Int. J. Remote Sensing 23:2631-2649.

Richter, R., Schläpfer, D., 2011. Atmospheric / Topographic Correction for Airborne Imagery (ATCOR-4 User Guide, Version 6.0.2, August 2011). - DLR report DLR-IB 565-02/11, Wessling, Germany, 194p. Available from http://www.rese.ch/download/

Ryan, R.E., Pagnutti, M, 2009. Enhanced Absolute and Relative Radiometric Calibration for Digital Aerial Cameras. In: Fritsch, D., (Ed.), Photogrammetric Week 2009, Wichmann Verlag, Heidelberg, Germany, pp. 81-90.

Schaepman-Strub, G., Schaepman M.E., Painter, T.H., Dangel, S., Martonchik, J.V, 2006. Reflectance quantities in optical remote sensing—definitions and case studies, Remote Sensing of Environment 103 (1), 27–42.

Schläpfer, D., Richter, R., Kellenberger, T., 2012. Atmospheric and topographic correction of photogrammetric airborne digital scanner data (ATCOR-ADS). International Calibration and Orientation Workshop EuroCOW 2012. Castelldefels (Barcelona), 8–10 Feb.

Schott, J.R., 2007. Remote sensing: The image chain approach. Oxford University Press, Inc. 2nd ed., 666 pages.

SMEAR, 2012. Smear research stations. http://www.atm.helsinki.fi/SMEAR/ (Accessed 27 July 2012)

Smith, G.M., Milton, E.J, 1999. The use of the empirical line method to calibrate remotely sensed data to reflectance. Remote Sensing 1999, 20, 2653-2662.

Song, J., Lu, D., and Weseley, M. L., 2003. A simplified atmospheric correction procedure for the normalized difference vegetation index. Photogrammetric Engineering & Remote Sensing, 69(5), pp. 521-528.

Suomalainen, J., Hakala, T., Peltoniemi, J., Puttonen, E., 2009. Polarised Multiangular Reflectance Measurements Using the Finnish Geodetic Institute Field Goniospectrometer. Sensors 9 (5), 3891-3907.

Talaya, J., Kornus, W., Alamús, R., Soler, E., Pla, M., Ruiz, A., 2008. Analyzing DMC performance in a production environment XXI ISPRS Congress. Beijing 3-11 July.

Vermote, E.F., Tanré, D., Deuzé, J.L., Herman M., and Morcrette, JJ., 1997. Second simulation of the satellite signal in the solar spectrum, 6S: an overview. IEEE Transactions on Geoscience and Remote Sensing, 35, 675-686, 1997.

von Schönermark M., Geiger, B., Röser, H.P., 2004. Reflection properties of vegetation and soil. Wissenschaft und Technik Verlag, Berlin. 352 pages.

UltraCam, 2012. http://www.microsoft.com/ultracam/en-us/default.aspx

Index of Figures

Index of Tables